MOLECULAR AND CELLULAR BIOLOGY, May 1995, p. 2547–2557 Vol. 15, No. 5
0270-7306/95/$04.00+0

Carcinogenic Nickel Silences Gene Expression by Chromatin Condensation and DNA Methylation: a New Model for Epigenetic Carcinogens

Y.-W. LEE, C. B. KLEIN, B. KARGACIN, K. SALNIKOW, J. KITAHARA, K. DOWJAT, A. ZHITKOVICH, N. T. CHRISTIE, AND M. COSTA*

Nelson Institute of Environmental Medicine and Kaplan Comprehensive Cancer Center, New York University Medical Center, New York, New York 10016

Received 16 December 1994/Returned for modification 9 February 1995/Accepted 15 February 1995

A transgenic *gpt*$^+$ Chinese hamster cell line (G12) was found to be susceptible to carcinogenic nickel-induced inactivation of *gpt* expression without mutagenesis or deletion of the transgene. Many nickel-induced 6-thioguanine-resistant variants spontaneously reverted to actively express *gpt*, as indicated by both reversion assays and direct enzyme measurements. Since reversion was enhanced in many of the nickel-induced variant cell lines following 24-h treatment with the demethylating agent 5-azacytidine, the involvement of DNA methylation in silencing *gpt* expression was suspected. This was confirmed by demonstrations of increased DNA methylation, as well as by evidence indicating condensed chromatin and heterochromatinization of the *gpt* integration site in 6-thioguanine-resistant cells. Upon reversion to active *gpt* expression, DNA methylation and condensation are lost. We propose that DNA condensation and methylation result in heterochromatinization of the *gpt* sequence with subsequent inheritance of the now silenced gene. This mechanism is supported by direct evidence showing that acute nickel treatment of cultured cells, and of isolated nuclei in vitro, can indeed facilitate *gpt* sequence-specific chromatin condensation. Epigenetic mechanisms have been implicated in the actions of some nonmutagenic carcinogens, and DNA methylation changes are now known to be important in carcinogenesis. This paper further supports the emerging theory that nickel is a human carcinogen that can alter gene expression by enhanced DNA methylation and compaction, rather than by mutagenic mechanisms.

Whereas nickel compounds are potent human and rodent carcinogens, they are generally not mutagenic in most classical bacterial or mammalian cell assays (2, 8, 36). Nickel compounds exhibit slight genotoxicity since they produce some small amount of DNA damage or genome alterations, including DNA-protein cross-links, DNA strand breaks, chromosomal aberrations, and sister chromatid exchanges in vitro and in isolated human peripheral lymphocytes, as well as in cultured mammalian cells (73; reviewed in reference 13). Carcinogenic nickel compounds selectively damage genetically inactive heterochromatic regions, which may explain their lack of mutagenicity despite obvious genotoxicity (13). They have also been shown to act synergistically with many other genotoxic or mutagenic carcinogens (67), suggesting that nickel is adding something that is not associated with mutagenesis during carcinogenesis. We have previously reported that water-insoluble Ni compounds (nickel sulfide, nickel subsulfide, and nickel oxides) yield very high levels of 6-thioguanine (6TG) resistance at the bacterial xanthine guanine phosphoribosyl transferase (GPT) locus (*gpt*) in Chinese hamster V79-derived G12 cells (14, 36, 48). In fact, this nickel-induced 6TG resistance was higher than any other mutagenic response observed to date in G12 cells. The G12 cells carry a single copy of *gpt*, the gene for a bacterial nucleotide salvage enzyme that is functionally analogous to the endogenous mammalian hypoxanthine phosphoribosyl transferase (HPRT) gene (*hprt*). It is useful to remember that *gpt* gene inactivation (*gpt*$^-$) is selected by resistance to 6TG, and gene reactivation (*gpt*$^+$) is selected by resistance to a mixture of 100 μM hypoxanthine, 1 μM aminopterin, and 100 μM thymidine (HAT) (42, 43). Since the *gpt* transgene in G12 cells is more readily mutated than *hprt* in the parental V79 cells (42, 43), it was thought that a mutagenic spectrum could finally be identified for nickel by using the sensitive G12 cell system.

The high incidence of 6TG resistance induced by nickel in the transgenic G12 cell line, but not in another transgenic cell line, G10 (36, 41), suggested that the location of the transgene in G12 cells near a large and dense heterochromatic region of the genome (43) is a preferential site for nickel activity. Since nickel was known to be clastogenic, we speculated that a high frequency of *gpt* deletions would be found. However, initial studies of numerous NiS- or Ni_3S_2-induced 6TG^R clones showed that the *gpt* sequence was not deleted, nor were coding region sequence mutations found (48). This was quite different from the *gpt* mutation spectrum described for other clastogens such as X rays and bleomycin (41). Although *gpt* transgene deletions following clastogen treatment of G12 cells are frequent (~50%) (41), deletions are not the only recovered mutations, and these cells can also be used to study mutations within the PCR-recoverable *gpt* gene. Both partial and total deletions, as well as point mutations (e.g., a T → G transversion in an X-ray mutant), have been identified for the *gpt* sequence in G12 cells as determined by PCR screening of several hundred spontaneous and clastogen-induced mutants (41).

With nickel, the high levels of acquired resistance to 6TG without *gpt* deletion in the G12 cells argued against true mutagenesis and suggested the possibility of gene silencing by epigenetic mechanisms involving DNA methylation. Such mechanisms had been found to be operative in silencing other transgenes, including *gpt*$^+$ or transgenic *hprt*$^+$ in various cell systems (25, 49, 50). The first evidence that nickel may operate

* Corresponding author. Mailing address: Nelson Institute of Environmental Medicine, New York University Medical Center, 550 First Ave., New York, NY 10016. Phone: (914) 351-2368 or (212) 263-5280. Fax: (914) 351-2118.

as an epigenetic carcinogen was derived from our earlier microcell chromosome transfer studies, in which restoration of nickel-inactivated gene activity was regained by the transfer of intact X chromosomes and could be modulated by growth of the X chromosome donor cells in 5-azacytidine (40). We have since cloned and identified several gene sequences, including those for thrombospondin and a heme-containing peroxidase, that are expressed in normal hamster cells but not in nickel-transformed hamster cells (19, 21, 69). In vitro chloramphenicol acetyltransferase assays employing vectors carrying different regions of the thrombospondin gene promoter have indeed shown that the expression of the thrombospondin gene is strikingly different in normal versus nickel-transformed cells (69), and new evidence suggests that this involves transcription factors that positively regulate this gene.

In this paper, we describe data showing that nickel specifically induced a 6TG-resistant phenotype in G12 variants that is due to reversible *gpt* transgene silencing involving DNA condensation and methylation. This mechanism of acquired 6TG resistance has not been identified for any other mutagen applied to these cells, nor is it a mechanism commonly involved in spontaneous *gpt* silencing (reviewed in Table 1). These findings are supported by Northern (RNA) blots and enzyme studies showing that *gpt* activity has been turned off by nickel yet restored to functional levels in HAT-resistant (*gpt*-expressing) revertants. We demonstrate that epigenetic processes are important in regulating *gpt* gene expression in the G12 cells as evidenced by increased DNA methylation detected at some sites within the *gpt* sequence and within the flanking regions in nickel-induced $6TG^R$ cells. These inherited changes in DNA methylation were found to correlate with increased DNase I and *Msp*I resistance, pointing to more condensed chromatin structure in the *gpt* region during transgene inactivation. Both DNA methylation and DNase I resistance are lost in the HAT revertants which reexpress *gpt*. Finally, we present evidence suggesting that the *gpt* transgene in nickel-induced $6TG^R$ variants has in fact become incorporated into heterochromatin, and we conclude with a mechanistic model whereby nickel induces an inherited heterochromatin spreading in the vicinity of the *gpt* transgene insertion site in G12 cells, thus silencing *gpt* expression. This proposed mechanism is supported by data showing that DNA condensation occurs temporally following acute nickel treatment of both cultured G12 cells and isolated nuclei in vitro. These important findings provide further evidence that nickel may be carcinogenic by virtue of its ability to heritably alter gene expression by nonmutagenic mechanisms, particularly in genomic regions that are sensitive to nickel activity. The model that is presented here may apply to other epigenetic carcinogens that yield heritable chromosomal changes without demonstrated mutagenic potential and may also have ramifications that are relevant to studies of transgene behavior in gene therapy protocols.

MATERIALS AND METHODS

Cell culture and generation of $6TG^R$ gpt^- variants. The gpt^+ transgenic G12 cells are cultured in F12 medium (Life Technologies, Inc., GIBCO BRL, Grand Island, N.Y.) supplemented with 5% fetal bovine serum (GIBCO) and 1% penicillin-streptomycin (GIBCO) at 37°C in a humid 5% CO_2 atmosphere (42, 43). In order to maintain a low spontaneous-mutant frequency, G12 cultures are supplemented with HAT, and fresh cultures are defrosted every 6 weeks. One day prior to the beginning of each mutagenesis experiment, the cells are removed from HAT selection. For optimum selection of $6TG^R$ variants, 10 μg of freshly prepared 6TG per ml is used. For the collection of pure, independent variant clones, only one clone is isolated per treated cell population. After initial growth of these cells in nonselective media, the clones are retested to confirm the $6TG^R$ HAT^S phenotype.

Reversion assays. The protocol used in the reversion studies was adapted from that previously used for selection of *hprt* reversion in V79 cells (74). Spontaneous revertants were purged from the cultures of nickel-induced $6TG^R$ variants by growing the cells in 6TG-supplemented media for several days and then culturing them in nonselective medium for 2 more days before the reversion assay was begun. For each $6TG^R$ variant clone, 5×10^5 cells were seeded into 80-cm^2 tissue culture flasks and exposed to 3 or 5 μM 5-azacytidine for 48 h. After the treatment was removed, the cells were rinsed with saline A or Earle's balanced salt solution and incubated for a 2-day recovery period. The cells were then replated at 10^3 to 10^4 cells into 10 dishes (100-mm diameter) containing HAT selection medium, and the revertant clones were grown for 12 days. Since epigenetic reversion frequencies are much higher (10^{-3}) than mutagenic reversion frequencies (10^{-6} to 10^{-7}), it is generally not necessary to plate more than 10^5 cells per experiment. In fact, we have found it optimal to seed only 10^4 cells per 100-mm-diameter HAT selection dish in the experiments with 5-azacytidine-induced reversion. When very low levels of reversion are expected, as with spontaneous $6TG^R$ variants, it is necessary to plate up to 10^5 to 10^6 cells per dish. HAT selection is not sensitive to cell density effects, as we have previously plated up to 10^6 cells per dish in mutagenic reversion studies (74). HAT^R colonies were stained with either Giemsa stain or crystal violet as previously reported (41, 43, 48). The reversion frequencies were calculated as the number of HAT^R colonies formed per 10^4 or 10^6 clonable cells seeded.

Enzyme analyses. We have measured GPT enzyme activity using a slightly modified HPRT assay protocol (23). This assay directly measures the formation of nanomoles of XMP per minute per milligram of protein and utilized [^{14}C]xanthine as the GPT substrate. For measurements of HPRT activity, [^{3}H]hypoxanthine was used as the substrate. Cell extracts were obtained by a freeze-thaw procedure, and the supernatants were stored at −70°C for later use. The 100-μl enzyme assay mix contained 50 mM Tris-HCl (pH 7.4), 5 mM $MgCl_2$, 5 mM 5-phosphorybosyl-1-PP_i, 1 μl of isotope (either [^{14}C]xanthine [34.5 Ci/mol] or [^{14}C]hypoxanthine [54 Ci/mol]), and 10 μg of protein extract. The assay mixture was incubated at 37°C for different time intervals. The zero point sample was kept on ice. Reactions were terminated by the addition of EDTA (100 mM), and the mixtures were applied to 25-mm-diameter DEAE filter discs (Whatman DE-81) on a Millipore sampling manifold. The filters were rinsed twice with Tris-HCl and dried. The radioactivity was quantitated by liquid scintillation counting. Enzyme activity was calculated from those portions of the activity curves in which the reaction rates were constant with the time.

DNA methylation studies. Five micrograms of DNA from G12 cells and several $6TG^R$ nickel-induced G12 variants was first digested with the restriction endonuclease *Eco*RV (5 U/μg of genomic DNA), extracted with phenol-chloroform, and ethanol precipitated. This digestion released a 1.7-kb genomic fragment containing ~780 bp of 5′ flanking sequences, the simian virus 40 regulatory region of the pSV2*gpt* plasmid, and a 580-bp portion of the *Escherichia coli gpt* sequence (63). This DNA fragment was resuspended with 10 μl of Tris-EDTA (pH 8.0) and digested again with 5 U of the methylation-sensitive restriction endonuclease *Hpa*II (5′-CCGG-3′; U.S. Biochemicals) or *Hae*II (5′-PuGC GCPy-3′; New England Biolabs) per μg of DNA. The digested DNA was fractionated on 1.0 or 1.2% agarose gels, blotted onto nylon membranes (BioTrace; Gelman Sciences), and hybridized with an appropriate radiolabeled probe.

DNase I and *Msp*I sensitivity assay. The procedure for the isolation of nuclei was modified from those reported previously (6, 38). Briefly, cells from one (15-cm-diameter) plate were washed twice with ice-cold phosphate-buffered saline (PBS; 8 g of NaCl, 0.2 g of KCl, 1.44 g of Na_2HPO_4, and 0.24 g of KH_2PO_4 in 1 liter, pH 7.4), scraped and pooled into PBS, and collected by centrifugation for 5 min at 1,125 × *g* and 4°C. The cell pellet was washed again with PBS, resuspended in 12 ml of cold lysis buffer (0.25 M sucrose, 20 mM Tris-Cl [pH 8.0], 5 mM $MgCl_2$, 1 mM phenylmethylsulfonyl fluoride, and 0.5% Triton X-100), and left on ice for 5 min. Cell lysates were homogenized by using a Dounce homogenizer (Weaton) with pestle A. The nuclei were pelleted (1,125 × *g*, 15 min, 4°C) and washed twice with washing buffer (the lysis buffer with neither Triton X-100 nor phenylmethylsulfonyl fluoride). Finally the nuclear pellets were resuspended in DNase I buffer (10 mM Tris-Cl [pH 7.4], 10 mM NaCl, 3 mM $MgCl_2$, and 100 μM $CaCl_2$) for 20 min of digestion at room temperature with increasing amounts of DNase I (0, 0.3, 0.6, 0.9, 1.2, and 1.5 U) or *Msp*I (0, 1, 5, and 20 U) in a reaction volume of 200 μl. The reactions were terminated by adding the same volume of stop solution (1% sodium dodecyl sulfate [SDS], 0.3 M NaCl, 50 mM Tris-Cl [pH 8.0], 50 mM EDTA) containing 1 mg of proteinase K per ml and incubating the mix at 55°C for 1 h. The DNase I- or *Msp*I-digested DNAs were extracted with phenol-chloroform and ethanol precipitated. The recovered and resuspended DNAs were then digested with an excess amount of *Eco*RV, separated on a 1.0% agarose gel, blotted, and hybridized with a 1,150-bp (*Hin*dIII-*Apa*I) fragment from pSV2*gpt* as the probe.

Isolation of heterochromatin and *gpt*-specific probing. Chromatin fractionation was performed essentially as previously described (65) with minor modifications. For each cell line (G12, G10, and nickel-induced variants) 10^8 cells were resuspended in 10 ml of buffer containing 0.25 M sucrose, 20 mM Tris (pH 8.0), 5 mM $CaCl_2$, 1 mM phenylmethylsulfonyl fluoride, and 0.5% Nonidet P-40. The cells were homogenized with a Dounce homogenizer using 10 strokes, and the released nuclei were collected by centrifugation at 1,000 × *g* for 5 min. The pelleted nuclei were resuspended in the same buffer and centrifuged again. Finally, the nuclei were washed once in buffer without detergent, resuspended at a density of ~5 to 6 mg/ml, and treated with 50 U of micrococcal nuclease (Boehringer Mannheim) per ml at 37°C for 10 min. The reaction was stopped by

the addition of 10 mM EDTA, and the samples were placed on ice. Nuclei were collected by centrifugation at 12,000 × *g* for 3 min, resuspended (supernatant from this step was saved) in 900 μl of Tris-EDTA buffer, and incubated on ice for 30 min. They were again centrifuged at 12,000 × g for 15 min. The supernatants from the first and second centrifugations were combined, and this fraction was denoted as soluble chromatin. This sample was further fractionated to obtain euchromatin- and heterochromatin-enriched fractions, by precipitation of the heterochromatin with an excess of salt. A 5 M solution of NaCl was added dropwise with constant mixing to a final concentration of 150 mM, and then each sample was immediately centrifuged at 12,000 × *g* for 20 min. The supernatant and precipitate from this final step represent euchromatin- and heterochromatin-enriched fractions, respectively. The efficiency of extraction of heterochromatic and euchromatic fractions was monitored at this point by assessing the quantity of histone H_1 by SDS-polyacrylamide gel electrophoresis (65). All preparations had equivalently high ratios of histone H_1 in the heterochromatin fraction compared with histone H_1 in euchromatin fraction.

To isolate and purify DNA from these fractions, first each fraction was treated with RNase (20 μg/ml, 37°C, 30 min), then the samples were adjusted to 0.5% SDS, and digestion with 200 μg of proteinase K per ml proceeded overnight at 37°C. The samples were phenol-chloroform extracted, and the DNA was precipitated with absolute ethanol containing 10 mM $MgCl_2$. The DNA was dissolved in Tris-EDTA buffer, and its concentration was determined spectrophotometrically.

To analyze these fractions for *gpt*-specific sequences, a series of six twofold dilutions (starting with 5 μg/ml) of heterochromatin DNA from each cell line was applied to a BA85 nitrocellulose membrane (Schleicher & Schuell, Keene, N.H.) by using a Minifold II slot blot apparatus (Schleicher & Schuell). Before loading, the DNA was denatured by 0.2 N NaOH and heated at 80°C for 10 min. The DNA was UV cross-linked to the membrane in a UV Stratalinker 1800 (Stratagene, La Jolla, Calif.) and prehybridized for 6 h at 65°C in hybridization solution containing 5× SSC (1× SSC is 0.15 M NaCl plus 0.015 M sodium citrate), 1× Denhardt's solution, 50 mM NaH_2PO_4 (pH 7.0), 5% dextran sulfate, and 50 μg of denatured salmon sperm DNA per ml. The *gpt* probe consisted of a 561-bp PCR product derived from pSV2*gpt* plasmid DNA, which contains the entire coding region of the *gpt* gene. The primer sequences and the conditions for the PCRs have been described in detail elsewhere (48). The PCR product was gel purified and labeled with [α-^{32}P]dATP (Amersham) by using a random primer labeling kit (Boehringer Mannheim). Hybridization was carried out overnight at 65°C in a roller hybridization incubator (Robins Scientific, Sunnyvale, Calif.). The membrane was washed three times in 0.1× SSC–0.1% SDS at 52°C before being processed for autoradiography. The autoradiograms were analyzed densitometrically. Each band on the film was quantitated with a Scanmaster 3+ (Howtek, Inc.) scanner, and the data were processed and analyzed by Bio Image System, Inc. (Millipore), computer software.

Gene-specific DNase I PCR. To study the acute effects of nickel treatment on *gpt*-specific cellular DNA in cultured G12 cells, we employed a DNase I PCR assay (61). Cells were treated with 2 μg of nickel subsulfide per cm^2 (the dose yielding 3% survival) for 16 h as previously reported (48). Following removal of the nickel subsulfide, nuclei were isolated after different recovery periods (0, 1, 2, 3, and 11 days), and DNA processing procedures were identical to those described above for DNase I sensitivity assays. In order to investigate the in vitro effects of nickel on chromatin structure, isolated nuclei from G12 cells were incubated with 200 μM $NiCl_2$ for 1 h on ice prior to digestion with DNase I. Under these conditions, nickel chloride did not directly inhibit DNase I activity as determined by a standard enzyme activity assay (39a). The digested DNAs were subjected to PCR using a specific *gpt* PCR primer set, 5′-AACACTTTT TAAGCCGTAGATAAA and 5′-TATTGTAACCCGCCTGAAGTTAAA, for amplifying the entire coding region of the gene (43, 48). For normalization of DNA quantitation and PCR conditions, coamplification of the β-globin gene was achieved with the primer set 5′-TGTTGAGTCACAAGCCCAGAAAC and 5′-AGGAGTGGATCACCTTCTTGCC. PCR products were radiolabeled by adding [α-^{32}P]dATP or [α-^{32}P]dCTP during the PCR and were analyzed by exposure to X-ray film following 4% polyacrylamide gel electrophoresis. For further analysis (see Tables 3 and 4), the band intensities on the films were quantitated by a computer scanner (ScanMaker IIXE; Microtek).

RESULTS

Lack of *gpt* transcription in nickel-induced 6TG-resistant variants of G12 cells. In several previous papers we have shown that clastogenic nickel compounds produced the highest frequency (10^{-3}) of 6TG-resistant colonies ever recovered from the transgenic G12 cell line (reviewed in Table 1). We have also demonstrated that deletion loss of the *gpt* transgene, which occurs spontaneously to varying extents in both the G12 and G10 cell lines and can be induced to even higher levels by X rays and bleomycin, is not generally induced by nickel (Table 1). Unlike the mutagenic spectrum found in previous studies, in which transgene deletions occurred in 20% of spontaneous

TABLE 1. Review of spontaneous and induced mutagenesis of the *gpt* transgene in G12 and G10 cells

Cell line	Mutagen	6TG^R mutagenesis[a] (reference[s])	*gpt* deletion frequency (%)[b]
G12	Spontaneous	30 (43)	~20
	Bleomycin (100 μg/ml, 1 h)	210 (43)	~50
	X rays (500 cGy)	510 (43)	~50
	Ni_3S_2 (0.3 μg/cm^2, 24 h)	1,370 (36, 48)	0
G10	Spontaneous	100 (43)	~50
	Bleomycin (100 μg/ml, 1 h)	1,400 (43)	~90
	X rays (500 cGy)	2,600 (43)	~90
	Ni_3S_2 (0.3 μg/cm^2, 24 h)	150 (36)	ND

[a] 6TG resistance is expressed as the number of mutants per 10^6 surviving cells, at an approximately 30% survival dose of all mutagens listed.
[b] As determined by PCR and Southern blot analysis of the *gpt* sequence. All data except results for Ni_3S_2 are reported in reference 44. ND, not determined.

G12 mutants and in about 50% of X-ray- and bleomycin-induced G12 mutants (41), preliminary evidence showed the *gpt* transgene to be intact and not mutated in the genome of most of the independent nickel-induced 6TG^R G12 cell lines (48). The transgene deletion frequencies induced in these experiments by insoluble crystalline nickel subsulfide (Ni_3S_2) and crystalline nickel sulfide (NiS), respectively, were 0% (0 of 24)

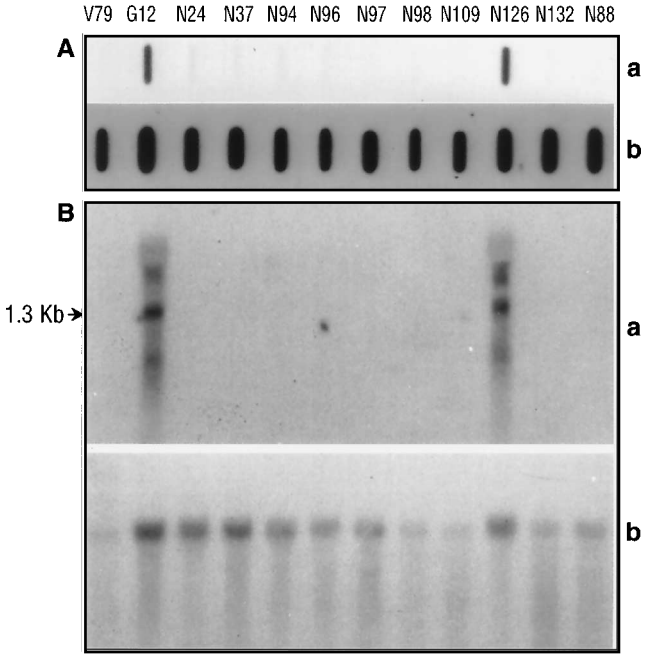

FIG. 1. Analyses of *gpt* transcription in several NiS- or Ni_3S_2-induced 6TG-resistant G12 variants. (A) Slot blot analyses of *gpt* transcripts. Seven micrograms of total RNA from each variant was denatured by a glyoxal-dimethyl sulfoxide method (70) and transferred to nylon membranes with a slot blot apparatus. The membranes were hybridized with a ^{32}P-labeled *gpt* probe (a) that was generated by random primer labeling of a 561-bp PCR product of the *gpt* coding sequence of pSV2*gpt*. To control for gel loading differences, the membranes were stripped and rehybridized with a β-actin probe (b). V79 is the parental Chinese hamster cell line which does not contain the *gpt* gene. G12 is the transgenic cell line derived from *hprt*$^-$ V79 by transfection with pSV2*gpt* (42). N24 to N94 are NiS-induced and N96 to N132 are Ni_3S_2-induced 6TG-resistant G12 variants. (B) Northern blot analyses of *gpt* transcription. The experimental procedures and probes are the same as those described above, except that 14 μg of total RNA per cell line was fractionated on 1% agarose gels. The arrow indicates the expected 1.3-kb *gpt* mRNA.

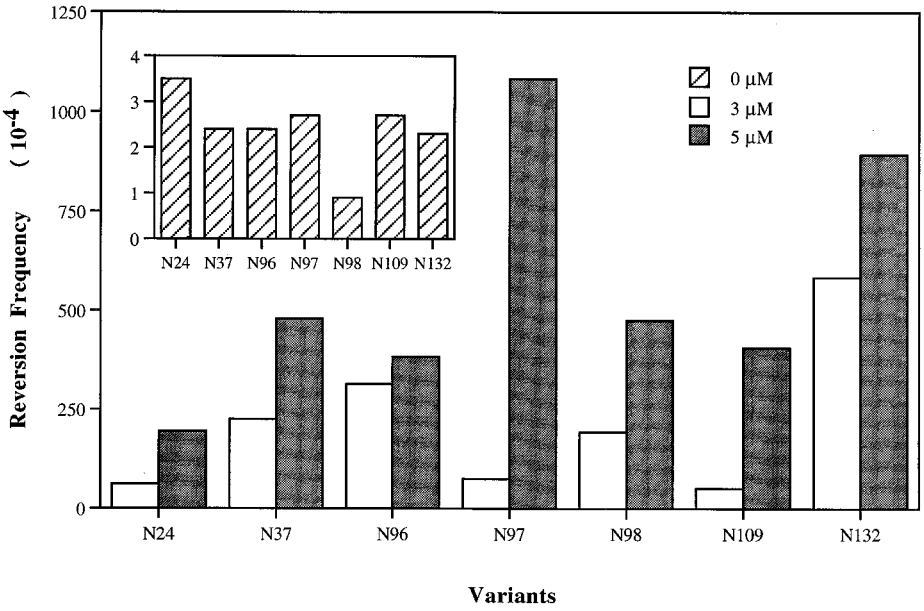

FIG. 2. 5-Azacytidine-induced reversion of nickel-induced 6TG-resistant G12 variants. Seven nickel-induced 6TG-resistant variant clones were reverted to HAT^R spontaneously (insert) or by 5-azacytidine at 3 μM (white bars) or 5 μM (black bars) as described in Materials and Methods. The identifications of the NiS- or Ni_3S_2-induced variants are the same as in Fig. 1.

and 3.6% (2 of 56), much less than the spontaneous G12 deletion frequency of about 20%. Furthermore, these carcinogenic nickel compounds never induced 6TG resistance more than threefold in the G10 cell line, which is much more highly prone to *gpt* deletion than G12 cells (Table 1). In summary, the predicted transgene deletion mechanism did not apply to the nickel compounds.

To examine the expression of *gpt* in numerous independently isolated NiS- or Ni_3S_2-induced $6TG^R$ clones for which we had previously shown that the *gpt* sequence was neither deleted nor mutated (48), we examined *gpt*-specific mRNA levels in several G12-derived cell lines (Fig. 1). These, and all mutant clones described here, were independently isolated from individually treated populations of cells. As clearly seen in both the slot blot (Fig. 1A) and Northern blot (Fig. 1B), only the untreated G12 cells and one nickel-induced $6TG^R$ clone (N126) exhibit a *gpt* transcript. In addition, we have examined slot blotted RNA of an additional 21 $6TG^R$ nickel-induced clones, finding *gpt* expression in only 1 other clone (47). These data show that treatment with carcinogenic nickel compounds can completely silence *gpt* expression in about 90% (27 of 31) of the independent $6TG^R$ cell lines that were isolated following nickel treatment of G12 cells.

Reversion of the 6TG-resistant phenotype spontaneously and with 5-azacytidine. Since *gpt* transgene expression may have been silenced in G12 cells by mechanisms involving DNA methylation rather than mutations or deletions, we investigated whether the gpt^- phenotype could be reverted to a gpt^+ phenotype. Figure 2 shows spontaneous and 5-azacytidine-induced reversion to HAT resistance for seven independent NiS- or Ni_3S_2-generated $6TG^R$ variants of G12 cells. The high frequencies of both spontaneous (10^{-4}) and 5-azacytidine-induced (10^{-2}) reversion of these nickel variants are slightly higher than those reported for the epigenetic reversion of *gpt* expression in spontaneous, UV-induced, and ethylmethanesulfonate-induced $6TG^R$ variants in other studies utilizing *gpt* transgenes (49). As noted in Fig. 2, cell line-dependent differences in reversion potential are exhibited. Increasing the concentration of 5-azacytidine from 3 to 5 μM resulted in even higher levels of reversion for all nickel-induced $6TG^R$ variants shown (Fig. 2). Both NiS- and Ni_3S_2-induced $6TG^R$ variants arise at approximately equal frequencies in G12 cells (36), and $6TG^R$ variants derived from either treatment protocol have been shown to be similarly revertible with and without azacytidine. Reversion to HAT^R, however, could not be demonstrated for occasional nickel-induced $6TG^R$ clones that have sustained either a rare *gpt* deletion (N88) or a putative promoter mutation (N126) (47). Among all the nickel variants analyzed to date, only 2 of 31 exhibited *gpt* deletion, and another 2 of 31 have putative mutations involving promoter sequences.

Lack of GPT enzyme activity. In order to provide further evidence that *gpt* expression was silenced by nickel in $6TG^R$ variants and reactivated in HAT^R revertants, enzyme analyses were performed. The data (Table 2) confirm that a constitutive level of HPRT activity is detectable only in the parental V79

TABLE 2. Enzyme activities in some nickel-induced $6TG^R$ variants and HAT^R revertants of G12 cells

Cell line	Phenotype	GPT sp act (nmol of XMP formed/min/mg of protein)[a]
V79 (*hprt*)	HAT^R	0
G12 (*gpt*)	HAT^R	1.12
G12 variants		
1	$6TG^R$	0
2	$6TG^R$	0
3	$6TG^R$	0
G12 revertants		
A	HAT^R	0.76
B	HAT^R	0.39

[a] Data represent the means from two independent experiments. Only V79 showed HPRT activity: 1.72 nmol of IMP formed per min per mg of protein.

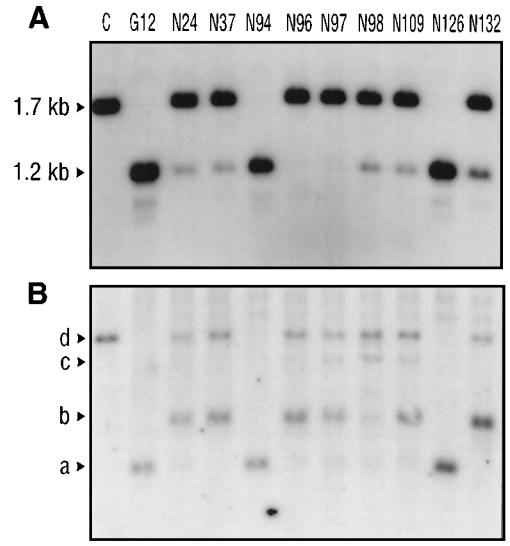

FIG. 3. Methylation of the *gpt* gene and its flanking sequence in nickel-induced 6TG-resistant G12 variants. (A and B) Five micrograms of the *Eco*RV-digested DNA was digested further with the methylation-sensitive restriction endonuclease *Hae*II (A) or *Hpa*II (B). The restriction fragments were hybridized with a 920-bp probe derived from the pSV2*gpt* plasmid (*Pvu*II-to-*Eco*RV fragment) as depicted in panel C. The variants are identified as in Fig. 1. Lane C contains *Eco*RV-digested G12 DNA.

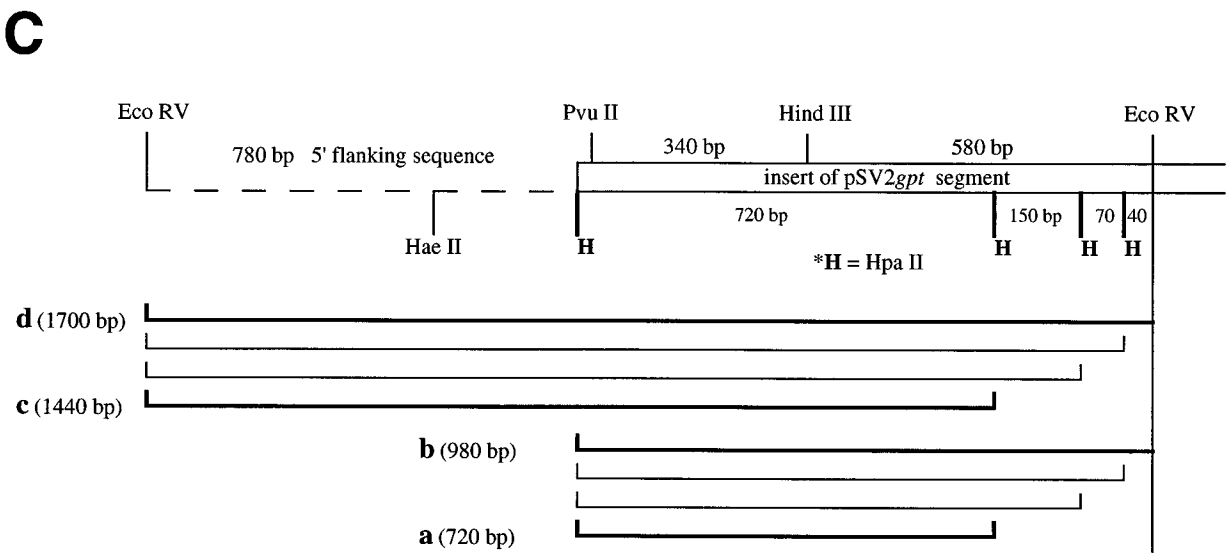

cells, whereas GPT activity conferred by the transgene is noted only in the *hprt*$^-$ *gpt*$^+$ G12 cells. Although both enzymes can recycle guanine, the enzymes exhibit species specificity for alternate substrates. The mammalian HPRT enzyme can utilize hypoxanthine but not xanthine, in contrast to the bacterial GPT enzyme, which can utilize xanthine. Thus, the experiments outlined in Table 2 utilized these specific enzyme substrates to measure both HPRT and GPT activities in the same cell lines. The table shows that GPT expression is unequivocally turned off in spontaneous 6TG^R G12 variant 1 and in the two nickel-induced variants 2 and 3 that were induced by Ni_3S_2 and NiO, respectively. There was no detectable reactivation of endogenous HPRT activity in any of these cell lines, thus proving that HPRT expression is permanently deficient in the V79 host cells used to create the G12 cell line (42). Reactivation of GPT activity did occur in the HAT^R revertant clones of 6TG^R variant 2, as shown in Table 2. These levels of enzyme recovery, 68 and 35% of the measured level of GPT in G12 cells, are similar to those that we and others have reported for HPRT recovery among HAT^R revertants of *N*-methyl-*N'*-nitro-*N*-nitrosoguanidine-induced 6TG^R V79 mutants (24, 74).

Evidence for DNA methylation in nickel-induced variants. We investigated whether *gpt* transgene silencing in G12 cells was associated with DNA hypermethylation following nickel treatment. The data in Fig. 3A show methylation patterns that are consistent with variable digestion of a *Hae*II restriction site (5′-PuGCGCPy-3′) in the 5′ flanking region of the *gpt* integration site in G12 cells. *Hae*II cuts this site when the internal C is not methylated. The location of this restriction site outside the coding region of the integrated *gpt* sequence is denoted in the partial G12 integration map shown in Fig. 3C. From other studies, it is known that this *Hae*II site is part of V79 host genome and not part of the integrated pVS2*gpt* plasmid which was partially deleted during integration (41, 47). In Fig. 3A, the DNA methylation patterns in nickel-induced 6TG^R variants N24, N37, N96, N97, N98, N109, and N132 clearly vary from that of untreated G12 cells, suggesting that DNA methylation changes at this site are associated with transgene silencing. Partial methylation of this site may be noted by the faint 1.2-kb bands shown in Fig. 3A for variants N24, N37, N98, N109, and N132. For two nonrevertible nickel-induced 6TG^R clones, N94 and N126, the DNA methylation patterns at this site do not

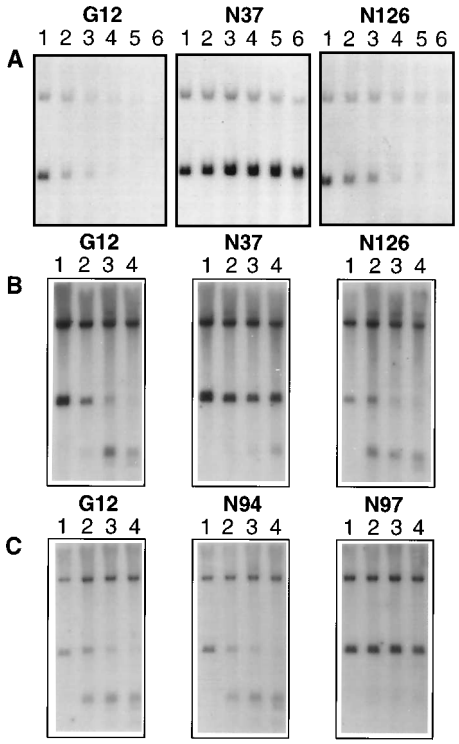

FIG. 4. Resistance of nickel-induced 6TG-resistant clones to DNase I and *Msp*I. (A) Nuclei isolated from G12, N37, and N126 cells were treated with 0, 0.3, 0.6, 0.9, 1.2, and 1.5 U of DNase I (lanes 1 to 6, respectively). Ten micrograms of the DNase I-digested DNA per lane was digested further with *Eco*RV to produce fragments, such that the upper (5.2-kb) and lower (1.7-kb) bands represent 3′ and 5′ genomic fragments, respectively. (B) The same cell lines as in panel A, but nuclei were treated with 0, 1, 5, and 20 U of *Msp*I (lanes 1 to 4, respectively) and 10 μg of DNA was digested again with *Eco*RV to produce the fragments shown. (C) Nonmethylated nickel-induced variant N94 and methylated variant N97 were analyzed for *Msp*I sensitivity as described for panel B.

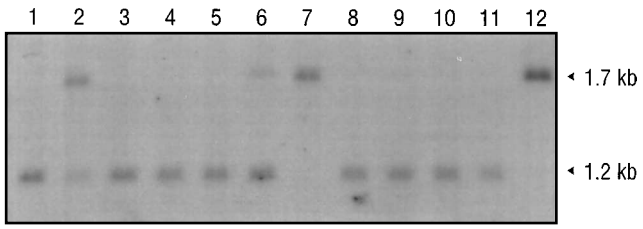

FIG. 5. Methylation patterns of the 5-azacytidine-revertible, nickel-induced 6TG^R variants (N37 and N97) and their HAT^R revertants induced by treatment with 5-azacytidine. The procedure for the methylation studies was the same as that described in the legend to Fig. 3. DNA samples from G12 (lanes 1 and 12), N37 (lane 2), four HAT^R revertants of N37 (lanes 3 to 6), N97 (lane 7), and four HAT^R revertants of N97 (lanes 8 to 11) were digested with *Eco*RV plus *Hae*II (lanes 1 to 11) or with *Eco*RV alone (lane 12). The methylation patterns in all but one of the HAT^R revertant clones (lane 6) show complete reversion to the pattern of unmethylated G12 DNA (lane 1).

differ from that of G12 cells (Fig. 3A), supporting the contention that true *gpt* gene mutations or promoter mutations may exist in these variant cell lines.

DNA methylation changes within the *gpt* coding sequence could also be detected in several nickel-induced 6TG^R variants with *Hpa*II (5′-CCGG-3′) digestion, as shown in Fig. 3B. The restriction map in Fig. 3C delineates numerous sites for *Hpa*II digestion within the integrated pSV2*gpt* sequence. Several predominant hybridization bands (e.g., 1.7, 1.4, 0.98, and 0.72 kb) are noted on the gel (Fig. 3B), as are several weaker bands corresponding to the alternate digests shown in Fig. 3C. It is clear that the same nickel-induced 6TG^R variants that showed *Hae*II methylation site changes in Fig. 3A also exhibited *Hpa*II site methylation changes within their pSV2*gpt* sequences. As with *Hae*II, *Hpa*II methylation patterns for the nonrevertible N94 and N126 variants do not differ from those for untreated G12 cells. Nickel seems to specifically alter DNA methylation of *gpt*, as to date 27 of 31 nickel-induced 6TG^R G12 clones have exhibited methylation pattern changes at these and other restriction enzyme sites (47).

Chromatin structure studies reveal DNase I and *Msp*I resistance. To study whether the observed changes in DNA methylation at several restriction enzyme sites in and around the integrated *gpt* sequence in G12 cells correlated with gross changes in the chromatin structure in this genomic region, DNase I sensitivity was examined in isolated nuclei from G12 cells and several nickel-treated variant cell lines (Fig. 4A). DNase I sensitivity or resistance is often studied as an indicator of chromatin openness or compaction within a gene-specific region of the genome (53, 56). It was noted that the revertible nickel-induced variant clone N37 (Fig. 4A) exhibited marked resistance to increasing concentrations of DNase I compared with that in the untreated G12 cells. In contrast, the nonrevertible and nonmethylated mutant N126 was not DNase I resistant compared with control G12 cells. In addition to the data in Fig. 4A, similar DNase I-resistant chromatin was exhibited by other revertible nickel variants (N97 and N132), whereas the nonrevertible variant N94 exhibits DNase I sensitivity identical to that of the parental G12 cells (47). Thus, in these experiments, DNase I resistance is coordinately demonstrated only in those mutants that also exhibit concurrent alterations in DNA methylation, as shown in Fig. 3A and B. Similarly, increased *Msp*I resistance has been noted in the same variants described above that demonstrate DNase I resistance (Fig. 4B), as well as in other variants (Fig. 4C; i.e., N94 nonmethylated variant and N97 methylated variant) (47). These results serve to illustrate the generality of increased chromatin compaction induced by carcinogenic nickel compounds with two different DNA-degrading enzymes and in a number of nickel-induced variants.

DNA methylation and chromatin structure in HAT^R revertants of nickel-induced variants. To test whether the altered methylation patterns and chromatin structures of the 6TG^R variants could be reversed to normal G12 patterns upon *gpt* reexpression, we isolated several HAT^R revertants derived from the nickel-induced 6TG^R variants N37 and N97 following treatment with 3 μM 5-azacytidine as described in Materials and Methods. As shown in Fig. 5, *Hae*II restriction patterns in the 5′ flanking region of the *gpt* integration site of the several HAT^R revertants derived from N37 (lane 3 to 5) and N97 (lanes 8 to 11) completely reverted to the G12 pattern (lane 1). Only one revertant of N37 (lane 6) showed partial reversion to yield a mixed methylation pattern. In addition, the methylation patterns derived with *Hpa*II in these revertants also showed complete reversion to the pattern previously noted for G12 cells (47). Furthermore, DNase I sensitivity of these HAT^R revertants was regained (47), indicating that DNA methylation and alterations of chromatin structure are coordinated events in this genome region. Thus, despite the fact that we have monitored DNA methylation only at very few limited sites in and around the *gpt* transgene, the hypermethylation observed in the nickel-induced 6TG^R variants and the subsequent loss of this methylation in HAT^R revertants were found to consis-

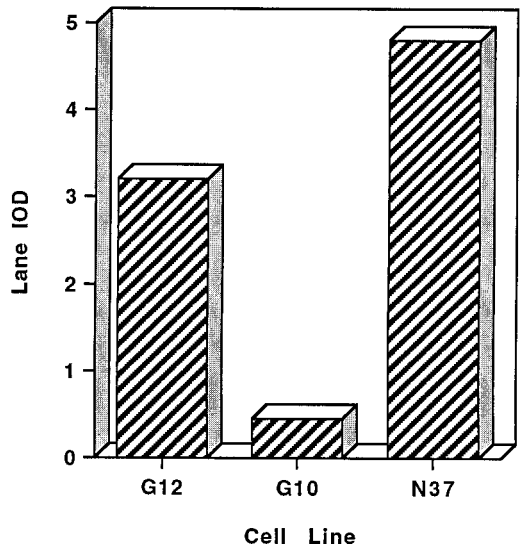

FIG. 6. Quantitation of *gpt* gene sequences in heterochromatin fractions of G12, G10, and a nickel-induced 6TG^R variant of G12. Heterochromatin-enriched fractions of each cell line were obtained, serially diluted, and slot blotted as described in Materials and Methods. Following hybridization with a ^{32}P-labeled *gpt* probe, the radioactivity on the blots was determined by densitometric analysis such that the optical density of each band was converted into an integrated optical density (IOD) per defined area. Each bar on the graph represents the sum of the IOD values for the series of dilution bands for each cell line indicated. The data represent the means from two independent experiments. Purity of the heterochromatin or euchromatin fractions was monitored by examining the content of histone H_1 by SDS-polyacrylamide gel electrophoresis (see Materials and Methods).

tently correlate with both DNase I sensitivity and gene expression.

Heterochromatin nature of the *gpt* region in G12 cells and nickel-induced variants. Since we are proposing that the *gpt* transgene in G12 cells becomes silenced by nickel treatment that compacts the chromatin, promotes DNA methylation, and may facilitate heterochromatin spreading to cover the transgene sequence, we investigated this possibility. Using heterochromatin isolated from G12 cells, G10 cells, and several nickel-induced G12 variants, we evaluated whether *gpt*-specific sequences could be found in this fraction. As shown in Fig. 6, G12 cells show significantly more *gpt* DNA in the heterochromatic fraction isolated by this procedure than observed for the non-nickel-sensitive G10 cells. This is consistent with cytogenetic analyses of fluorescent in situ hybridization of *gpt* probes. In G12 cells, the *gpt* integration site is evident on chromosome 1 (39b), which seen with appears to be proximal to an interstitial subtelomeric band of heterochromatin published C-banded karyotypes of Chinese hamster V79 cells (78). In contrast, the localization of *gpt* in G10 cells appears to be in the middle of the long arm of a much smaller autosome (possibly chromosome 6) (39b) that contains heterochromatin only in the centromere and accrocentric short arms (78). It is not surprising that the heterochromatin fractionation of G10 DNA pulls down some *gpt*-specific sequences, since the selective precipitation of heterochromatin from bulk chromatin by high salt is not absolute.

More important, however, are the data shown for the 6TG^R G12 nickel variant N37. As seen in Fig. 6, this cell line clearly demonstrates an even larger proportion of heterochromatin-associated *gpt*-specific DNA than the parental G12 cells. This result supports our hypothesis that heterochromatinization of certain DNA sequences can follow nickel exposure and is consistent with our other data showing DNA methylation and compaction. These studies, however, draw no conclusions as to the temporality of these events. Thus, the precise order of DNA compaction, DNA methylation, and heterochromatin spreading following nickel exposure is unknown.

TABLE 3. Quantitation of chromatin condensation following acute treatment of G12 cells with Ni_3S_2[a]

Time following treatment (days)	Chromatin condensation (% of control value)		
	In expt 1	In expt 2	Mean
0	66	113	90
1	75	236	156
2	167	328	248
3	197	262	230
11	431	ND[b]	431[c]

[a] DNA samples were coamplified with two primer sets that were specific for *gpt* and β-globin genes. Control DNA was amplified from untreated G12 cells. The other samples were amplified from G12 DNA and recovered from cells at various time intervals following an initial 16-h treatment with 2.0 μg of Ni_3S_2 per cm^2. Band intensities on the X-ray film were quantitated by ScanMaker IIXE from Microtek.
[b] ND, not done.
[c] Only from experiment 1.

Acute nickel treatments induce immediate DNA condensation in cells and in vitro. As a final demonstration that nickel can indeed provoke chromatin condensation consistent with our proposed model of transgene silencing, we show (Table 3) that acute treatment of cultured G12 cells with Ni_3S_2 yields measurable time-dependent increases in condensation of *gpt* sequence-specific cellular DNA derived from nickel-treated, but unselected, populations of G12 cells. Thus, early effects (within the first 3 days after nickel exposure) have been quantitated by a sensitive DNase I PCR method that effectively eliminates the 2- to 3-week delay in selecting *gpt*-silenced colonies by 6TG. Furthermore, immediate DNA condensation can even be detected and quantitated by this method in the DNA of isolated G12 nuclei treated with nickel for 1 h in vitro, as seen in Table 4. This effect is not induced at the same *gpt* sequence location in the G10 cellular DNA, consistent with our previous data (36) showing that the *gpt* sequence in G10 cells is also not significantly mutable or silenced by nickel compounds (Table 1).

DISCUSSION

As shown in this paper, highly carcinogenic insoluble nickel compounds have the capacity to inactivate the transcription of a stably integrated reporter transgene by inducing DNA methylation and compaction. As a result, we suggest that the gene becomes engulfed by the spreading of nearby heterochromatin

TABLE 4. Immediate effects of $NiCl_2$ on *gpt*-specific chromatin condensation in vitro

Cell line	Treatment	% of initial density[a] with:	
		0.125 U of DNase I	0.5 U of DNase I
G12	Untreated	73.9 ± 11.4	38.6 ± 1.8
	$NiCl_2$	82.1 ± 14.9	70.5 ± 4.3[b]
G10	Untreated	82.0 ± 2.9	57.4 ± 4.0
	$NiCl_2$	89.2 ± 15.8	54.0 ± 2.3

[a] The data represent the means ± standard deviations of three determinations from three separate PCRs.
[b] Significantly different from untreated ($P < 0.001$, Student's t test).

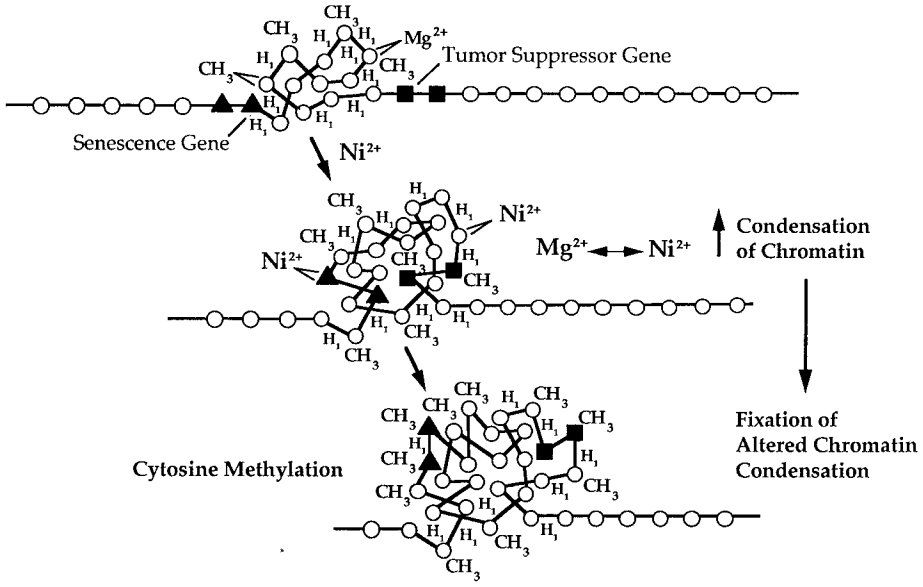

FIG. 7. Gene silencing model in which nickel-induced increases in heterochromatin condensation and hypermethylation of DNA may cause inherited inactivation of critical tumor suppressor or senescence genes. Cancer-relevant genes, such as tumor suppressors (black squares) and senescence genes (black triangles), may become incorporated into heterochromatin that is seeded by nickel-induced DNA condensation (middle panel) and stabilized by subsequent DNA methylation (bottom panel).

(Fig. 7) and is thus heritably silenced for subsequent generations. These findings are important since nickel compounds are carcinogenic but have not been found to be mutagenic in most mammalian cell assays. Thus, until now, it was not known how nickel could alter gene expression. The silencing of tumor suppressor genes, whether by physical deletion yielding allelic loss (80) or by genetic silencing involving DNA methylation (45) and DNA imprinting (22), is now recognized as an important feature of the carcinogenic process.

Gene silencing involving DNA methylation has been reported for numerous developmentally silenced endogenous genes (reviewed in references 9 and 12), for the inactive X chromosome (55, 66), and for constitutively expressed housekeeping genes such as those for thymidine kinase (*tk*) (28) and adenine phosphoribosyltransferase (*aprt*) (17). In addition, DNA methylation and gene inactivation have also been associated with heritable human disease, such as fragile X mental retardation (27, 75), and with human cancers involving silencing of tumor suppressor genes such as that for retinoblastoma (Rb) (26, 57, 68), a Wilm's tumor gene (H19) (83), and the von Hippel-Lindau tumor suppressor gene in renal carcinoma (30). It is well established that chromosomally integrated transgenes in transfected cell lines and in transgenic animals are susceptible to inactivation by changes in chromatin structure and/or DNA methylation (1, 20, 76). This was first reported for the transfected herpes simplex virus thymidine kinase gene in rodent (58, 60) and human (77) cells and has similarly been demonstrated for *gpt* silencing in several spontaneous, UV-induced, and chemically induced $6TG^R$ variants of transgenic human fibroblast cells (25, 49). In several human lymphoblastoid cell lines carrying stably transfected *hprt* cDNA in different locations of their genomes (50), the transgenic *hprt* was also demonstrated to be silenced by methylation rather than by mutation. This is analogous to the situation that we have described for the G12 versus G10 Chinese hamster cells, in which only the G12 cells appear to be affected by nickel-induced DNA methylation (41, 43). This may in part be explained by chromosome position effect, in which the expression of a transgene is modulated by the chromosomal environment into which it has integrated (1).

By fluorescent in situ hybridization, we have observed that the *gpt* plasmid has integrated in the nickel-responsive G12 cells into a site on chromosome 1 (39b) that is proximal to an interstitial subtelomeric band of dense constitutive heterochromatin identified in V79 karyotypes (78). This turns out to be very important, since nickel exerts its clastogenic and sister chromatid exchange effects with preferential reactivity toward condensed dense regions of heterochromatin (73), as confirmed in studies of Chinese hamster and mouse cells (72). In Chinese hamster cells, constitutive heterochromatin is localized in subtelomeric bands of both arms of chromosome 1; in the long arm of the X chromosome; the entire 9, 10, and Y chromosomes; the short arm of chromosome 8; and the centromeres of chromosomes 3 through 10 (5, 32). The concentrated heterochromatin of the long arm of the hamster X chromosome has been the focus of several studies showing this region to be a hot spot for both $NiCl_2$- and NiS-induced decondensation and damage, including frequent deletions (15). The X chromosome has also been identified to bear an epigenetically regulated senescence gene that can be silenced by carcinogenic nickel compounds (40). The localization of the *gpt* sequence in the vicinity of a large and dense heterochromatin region in G12 cells has been proposed to explain the selective sensitivity of this sequence to nickel modulation of its expression (43). In contrast, another transgenic cell line, G10, shows no significant response to nickel (Table 1) (36), and the *gpt* sequence in these cells appears to be localized far from any dense heterochromatin region in the middle of chromosome 6 (39b). Likewise, the *hprt* gene on the short arm of the X chromosome of V79 cells (23) is distant from the heterochromatic long arm, and this gene has also been shown to be only weakly responsive to nickel (reviewed in reference 36).

Heterochromatin is compacted DNA that is distinguished by several features, including minimal gene activity, a tightly compacted structure, late replication during the S phase of the cell cycle, and in the case of classically defined constitutive hetero-

chromatin, a high content of repetitive DNA sequences (16). Despite its general inactivity, some highly essential expressed genes, such as ribosomal genes, are known to reside in heterochromatin (16). Aberrant DNA methylation of CpG islands and heterochromatinization of these DNA regions are coordinated events that have been associated with cellular differentiation (54) and with cellular immortality and oncogenic transformation (64). We propose that nickel-induced chromatin condensation at euchromatin-heterochromatin junctions may cause actively expressed genes, such as the model *gpt* gene in G12 cells, to become incorporated into regions of spreading heterochromatin under conditions that favor DNA condensation. The G12 *gpt*-silencing mechanism presented here may be envisioned to also occur for a senescence gene or a tumor suppressor gene whose chromosomal location is either within heterochromatin or juxtaposed near heterochromatin or other condensed DNA. Recently, the spreading of an inactive (*Msp*I-resistant) chromatin conformation from a methylated region to an adjacent nonmethylated region of a plasmid reporter gene construct was directly shown to inhibit reporter gene expression (38). Position effect variegation, involving heterochromatin spreading and resulting gene silencing, has been well characterized in drosophilas (29, 37). However, the mechanisms involved in heterochromatin spreading and stabilization in drosophilas are likely to differ significantly from other eukaryotic systems, since *Drosophila* DNA is generally not methylated (59).

A unique feature of nickel carcinogenesis that is illustrated in the present study is that nickel may induce hypermethylation and DNA condensation in certain nickel-responsive genome regions. How does nickel induce this hypermethylation and induce changes in chromatin conformation? We propose that it is an indirect effect, whereby nickel may first induce chromatin condensation as shown herein (Tables 3 and 4). Nickel has previously been shown to increase chromatin condensation and is much more effective than Mg^{2+} in this regard (10, 81). Because the insoluble nickel particles used in this study are actively phagocytized by the G12 cells (36) and are dissolved in the proximity of the nuclear matrix (18), nickel ion concentrations may in fact be locally quite high in certain nuclear matrix-associated genome locales. In support of this, we have recently shown the perinuclear localization of nickel-induced oxidation as detected by photomicroscopy with fluorescent dichlorofluorescein (33, 35). DNA condensation could be seeded directly by the nickel ions or by their interactions with histones which are usually concentrated in condensed, nontranscribed DNA (46, 62). Indeed, we have recently confirmed a higher concentration of histone H_1 in heterochromatin than in euchromatin of Chinese hamster cells, and in fact the high histone H_1 ratios in heterochromatin versus euchromatin are markers of purity of such fractions (34). In addition, nickel has been reported to induce Z-DNA conformation (11), which is often stabilized by supercoiling and DNA methylation (7).

Following DNA condensation, as described above and depicted in Fig. 7, DNA methylases may recognize newly heterochromatic but unmethylated DNA and would de novo methylate this DNA. In support of this scenario, evidence from several studies suggests that DNA methylation is secondary to changes in chromatin structure (71, 82). Methylation of *hprt* on the inactive X chromosome, for example, has been demonstrated to occur after chromosome inactivation (52). Thus, while it is well established that methylated DNA often assumes an inactive chromatin structure (3, 4, 39), it also seems that inactive chromatin can be subsequently methylated. Once transiently incorporated into heterochromatin, senescence or tumor suppressor genes, like *gpt*, may become fully methylated, and these silenced genes may then be transmitted as such to daughter cells since established methylation patterns are generally heritable (31). The dynamics of DNA methylation versus inactivation appear to be complex, and although we have also not yet established the temporal order in which DNA compaction and methylation occur at the *gpt* locus in G12 cells, ongoing experiments should provide some answers in the near future.

We have recently reported that in nickel-transformed human HOS cells, the Rb gene is underexpressed and hypophosphorylated and lacks functional activity (51). As with the silencing of *gpt* in G12 cells, we have not identified Rb sequence mutations to be responsible for these effects, and DNA methylation is known to be capable of inactivating Rb expression (26, 68). We have also demonstrated that the thrombospondin gene, for which silencing of its antiangiogenic activity may be crucial for tumor development, is down-regulated in nickel-transformed Chinese hamster cells (69). Further studies are ongoing to establish the involvement of DNA condensation or methylation in either Rb or thrombospondin regulation.

In conclusion, whereas nickel compounds have also been shown to produce oxidative damage in cells (33, 35, 79) and we recently showed that this occurs preferentially in heterochromatin (34), nickel compounds have not been shown to be classically mutagenic to an extent that is commensurate with their carcinogenicity. In contrast, the gene-silencing mechanism described here to involve DNA compaction and methylation, while not envisioned to be the only mechanism involved in nickel carcinogenesis, is nevertheless a novel mechanism that may impart significant carcinogenic impact and may also be applied to other nonmutagenic carcinogens.

ACKNOWLEDGMENTS

This work was supported by grants ES 00260, ES 04895, ES 05512, and ES 04715 from the National Institute of Environmental Health Sciences and NCI/NIH grant CA 16087 (Kaplan Comprehensive Cancer Center).

REFERENCES

1. **Al-Shawi, R., J. Kinnaird, J. Burke, and J. O. Bishop.** 1990. Expression of a foreign gene in a line of transgenic mice is modulated by a chromosomal position effect. Mol. Cell. Biol. **10:**1192–1198.
2. **Amacher, D. E., and S. C. Paillet.** 1980. Induction of trifluorothymidine-resistant mutants by metal ions in L5178Y/TK$^{+/-}$ cells. Mutat. Res. **78:**279–288.
3. **Antequera, F., J. Boyes, and A. Bird.** 1990. High levels of *de novo* methylation and altered chromatin structure at CpG islands in cell lines. Cell **62:**503–514.
4. **Antequera, F., D. Macleod, and A. P. Bird.** 1989. Specific protection of methylated CpGs in mammalian nuclei. Cell **58:**509–517.
5. **Arrighi, F. E., T. C. Hsu, S. Pathak, and H. Sawanda.** 1974. The sex chromosomes of the Chinese hamster: constitutive heterochromatin deficient in repetitive DNA sequences. Cytogen. Cell Genet. **13:**269–274.
6. **Becker, P., R. Renkawitz, and G. Schutz.** 1984. Tissue-specific DNaseI hypersensitive sites in the 5′-flanking sequences of the tryptophan oxygenase and the tyrosine aminotransferase genes. EMBO J. **3:**2015–2020.
7. **Behe, M., and G. Felsenfeld.** 1981. Effects of methylation on a synthetic polynucleotide: the B–Z transition in poly(dG-m5dC) · poly(dG-m5dC). Proc. Natl. Acad. Sci. USA **78:**1619–1623.
8. **Biggart, N. W., and M. Costa.** 1986. Assessment of the uptake and mutagenicity of nickel chloride in salmonella tester strains. Mutat. Res. **175:**209–215.
9. **Bird, A.** 1992. The essentials of DNA methylation. Cell **70:**5–8.
10. **Borochov, N., J. Ausio, and H. Eisenberg.** 1984. Interaction and conformational changes of chromatin with divalent ions. Nucleic Acids Res. **12:**3089–3096.
11. **Bourtayre, P., L. Pizzorni, J. Liquier, J. Taboury, E. Taillandier, and J. F. Labarre.** 1984. Z-form induction of DNA by carcinogenic nickel compounds: an optical spectroscopic study, p. 227–234. *In* F. W. J. Sunderman (ed.), Nickel in the human environment, vol. 53. Oxford University Press, New York.
12. **Cedar, H., and A. Razin.** 1990. DNA methylation and development. Biochim. Biophys. Acta **1049:**1–8.

13. **Christie, N., and S. P. Katsifis.** 1990. Nickel carcinogenesis, p. 95–128. *In* E. C. Foulkes (ed.), Biological effects of heavy metals, vol. II. CRC Press, Inc., Boca Raton, Fla.
14. **Christie, N. T., D. Tummolo, C. Klein, and T. Rossman.** 1992. The role of Ni(II) in mutation, p. 305–317. *In* E. Nieboer and J. Nriagu (ed.), Nickel and human health: current perspectives. John Wiley & Sons, Inc., New York.
15. **Conway, K., and M. Costa.** 1989. Nonrandom chromosomal alterations in nickel-transformed Chinese hamster embryo cells. Cancer Res. **49:**6032–6038.
16. **Cook, K. R., and G. H. Karpen.** 1994. A rosy future for heterochromatin. Proc. Natl. Acad. Sci. USA **91:**5219–5221.
17. **Cooper, G. E., N. H. Khattar, P. L. Bishop, and M. S. Turker.** 1992. At least two distinct epigenetic mechanisms are correlated with high-frequency "switching" for APRT phenotypic expression in mouse embryonal carcinoma stem cells. Somat. Cell Mol. Genet. **18:**215–225.
18. **Costa, M.** 1991. Molecular mechanisms of nickel carcinogenesis. Annu. Rev. Pharmacol. Toxicol. **31:**321–337.
19. **Costa, M., Z. Zhuang, X. Huang, S. Cosentino, C. B. Klein, and K. Salnikow.** 1994. Molecular mechanisms of nickel carcinogenesis. Sci. Total Environ. **148:**191–199.
20. **Davies, R. L., S. Fuhrer-Krusi, and R. S. Kucherlapati.** 1982. Modulation of transfected gene expression mediated by changes in chromatin structure. Cell **31:**521–529.
21. **Dowjat, K., X. Huang, S. Consentino, and M. Costa.** Submitted for publication.
22. **Feinberg, A. P.** 1993. Genomic imprinting and gene activation in cancer. Nature Genet. **4:**110–113.
23. **Fenwick, R. G.** 1980. Reversion of mutation affecting the molecular weight of HGPRT: intragenic suppression and localization of the X-linked genes. Somat. Cell Genet. **6:**477–494.
24. **Fox, M., B. J. Rossiter, and J. Brennand.** 1988. Different mechanisms of reversion of HPRT-deficient V79 Chinese hamster cells. Mutagenesis **3:**15–21.
25. **Gebara, M. M., C. Drevon, S. A. Harcourt, H. Steingrimsdottir, M. R. James, J. F. Burke, C. F. Arlett, and A. R. Lehmann.** 1987. Inactivation of a transfected gene in human fibroblasts can occur by deletion, amplification, phenotypic switching, or methylation. Mol. Cell. Biol. **7:**1459–1464.
26. **Gregor, V., N. Debus, D. Lohmann, W. Hopping, E. Passarge, and B. Hortsthemke.** 1994. Frequency and parental origin of hypermethylated RB1 alleles in retinoblastoma. Hum. Genet. **94:**491–496.
27. **Hansen, R. S., S. M. Gartler, C. R. Scott, S. H. Chen, and C. D. Laird.** 1992. Methylation analysis of CGG sites in the CpG island of the human FMR1 gene. Hum. Mol. Genet. **1:**571–578.
28. **Harris, M.** 1982. Induction of thymidine kinase in enzyme-deficient Chinese hamster cells. Cell **29:**483–492.
29. **Henikoff, S., K. Loughney, and T. D. Dreesen.** 1993. The enigma of dominant position-effect variegation in Drosophila, p. 183–196. *In* J. S. Heslop-Harrison (ed.), The chromosome. BIOS Scientific Publishers, Oxford.
30. **Herman, J. G., F. Latif, Y. K. Weng, M. I. Lerman, B. Zbar, S. Liu, D. Samid, D. S. R. Duan, J. R. Gnarra, W. M. Linehan, and S. B. Baylin.** 1994. Silencing of the VHL tumor-suppressor gene by DNA methylation in renal carcinoma. Proc. Natl. Acad. Sci. USA **91:**9700–9704.
31. **Holliday, R.** 1987. The inheritance of epigenetic defects. Science **238:**163–170.
32. **Hsu, T. C., and F. E. Arrighi.** 1971. Distribution of constitutive heterochromatin in mammalian chromosomes. Chromosoma **34:**243–253.
33. **Huang, X., K. Frenkel, C. B. Klein, and M. Costa.** 1993. Nickel induces increased oxidants in intact cultured mammalian cells as detected by dichlorofluorescein fluorescence. Toxicol. Appl. Pharmacol. **120:**29–36.
34. **Huang, X., J. Kitahara, A. Zhitkovich, K. Dowjat, and M. Costa.** Submitted for publication.
35. **Huang, X., C. B. Klein, and M. Costa.** 1994. Crystalline Ni_3S_2 specifically enhances the formation of oxidants in the nuclei of CHO cells as detected by dichlorofluorescein. Carcinogenesis **15:**545–548.
36. **Kargacin, B., C. B. Klein, and M. Costa.** 1993. Mutagenic responses of nickel oxides and nickel sulfides in Chinese hamster V79 cell lines at the xanthine-guanine phosphoribosyl transferase locus. Mutat. Res. **300:**63–72.
37. **Karpen, G. H.** 1994. Position-effect variegation and the new biology of heterochromatin. Curr. Opin. Genet. Dev. **4:**281–291.
38. **Kass, S. U., J. P. Goddard, and R. L. Adams.** 1993. Inactive chromatin spreads from a focus of methylation. Mol. Cell. Biol. **13:**7372–7379.
39. **Keshet, I., J. Lieman-Hurwitz, and H. Cedar.** 1986. DNA methylation affects the formation of active chromatin. Cell **44:**535–543.
39a. **Kitahara, J.** Unpublished data.
39b. **Klein, C. B.** Unpublished data.
40. **Klein, C. B., K. Conway, X. W. Wang, R. K. Bhamra, X. H. Lin, M. D. Cohen, L. Annab, J. C. Barrett, and M. Costa.** 1991. Senescence of nickel-transformed cells by an X chromosome: possible epigenetic control. Science **251:**796–799.
41. **Klein, C. B., B. K. Kargacin, S. Cosentino, E. T. Snow, and M. Costa.** 1994. Metal mutagenesis in transgenic Chinese hamster cell lines. Environ. Health Perspect. **102:**63–67.
42. **Klein, C. B., and T. G. Rossman.** 1990. Transgenic Chinese hamster V79 cell lines which exhibit variable levels of *gpt* mutagenesis. Environ. Mol. Mutagen. **16:**1–12.
43. **Klein, C. B., L. Su, T. G. Rossman, and E. T. Snow.** 1994. Transgenic gpt^+ V79 cell lines differ in their mutagenic response to clastogens. Mutat. Res. **304:**217–228.
44. **Klein, C. B., L. Su, and E. T. Snow.** Submitted for publication.
45. **Laird, P. W., and R. Jaenisch.** 1994. DNA methylation and cancer. Hum. Mol. Genet. **3:**1487–1495.
46. **Laybourn, P. J., and J. T. Kadonaga.** 1991. Role of nucleosomal cores and histone H1 in regulation of transcription by RNA polymerase II. Science **254:**238–245.
47. **Lee, Y.-W.** 1995. Ph.D. thesis. New York University, New York.
48. **Lee, Y.-W., C. Pons, D. M. Tummolo, C. B. Klein, T. G. Rossman, and N. T. Christie.** 1993. Mutagenicity of soluble and insoluble nickel compounds at the *gpt* locus in G12 Chinese hamster cells. Environ. Mol. Mutagen. **21:**365–371.
49. **Lehmann, A. R., C. F. Arlett, S. A. Harcourt, H. Steingrimsdottir, and M. M. Gebara.** 1989. Mutagenic treatments result in inactivation of expression of a transfected bacterial gene integrated into a human cell line. Mutat. Res. **220:**255–262.
50. **Lichtenauer-Kaligis, E. G., J. Thijssen, H. den Dulk, P. van de Putte, J. G. Tasseron-de Jong, and M. Giphart-Gassler.** 1993. Genome wide spontaneous mutation in human cells determined by the spectrum of mutations in *hprt* cDNA genes. Mutagenesis **8:**207–220.
51. **Lin, X., W. K. Dowjat, and M. Costa.** 1994. Nickel-induced transformation of human cells causes loss of the phosphorylation of the retinoblastoma protein. Cancer Res. **54:**2751–2754.
52. **Lock, L. F., N. Takagi, and G. R. Martin.** 1987. Methylation of the Hprt gene on the inactive X occurs after chromosome inactivation. Cell **48:**39–46.
53. **Lois, R., L. Freeman, B. Villeponteau, and H. G. Martinson.** 1990. Active β-globin gene transcription occurs in methylated, DNase I-resistant chromatin of nonerythroid chicken cells. Mol. Cell. Biol. **10:**16–27.
54. **Lubbert, M., C. W. Miller, and H. P. Koeffler.** 1991. Changes of DNA methylation and chromatin structure in the human myeloperoxidase gene during myeloid differentiation. Blood **78:**345–356.
55. **Lyon, M. F.** 1992. Some milestones in the history of X-chromosome inactivation. Annu. Rev. Genet. **26:**16–28.
56. **Nitsch, D., A. F. Stewart, M. Boshart, R. Mestril, F. Weih, and G. Schutz.** 1990. Chromatin structures of the rat tyrosine aminotransferase gene relate to the function of its *cis*-acting elements. Mol. Cell. Biol. **10:**3334–3342.
57. **Ohtani-Fujita, N., T. Fujita, A. Aoike, N. E. Osifchin, P. D. Robbins, and T. Sakai.** 1993. CpG methylation inactivates the promoter activity of the human retinoblastoma tumor-suppressor gene. Oncogene **8:**1063–1067.
58. **Ostrander, M., S. Vogel, and S. Silverstein.** 1982. Phenotypic switching in cells transformed with the herpes simplex virus thymidine kinase gene. Mol. Cell. Biol. **2:**708–714.
59. **Patel, C. V., and K. P. Gopinathan.** 1987. Determination of trace amounts of 5-methylcytosine in DNA by reverse-phase high-performance liquid chromatography. Anal. Biochem. **164:**164–169.
60. **Pellicer, A., D. Robins, B. Wold, R. Sweet, J. Jackson, I. Lowy, J. M. Roberts, G. K. Sim, S. Silverstein, and R. Axel.** 1980. Altering genotype and phenotype by DNA-mediated gene transfer. Science **209:**1414–1422.
61. **Pikaart, M., J. Feng, and B. Villeponteau.** 1992. The polyomavirus enhancer activates chromatin accessibility on integration into the *HPRT* gene. Mol. Cell. Biol. **12:**5785–5792.
62. **Postnikov, Y. V., V. V. Shick, A. V. Belyavsky, K. R. Khrapko, K. L. Brodolin, T. A. Nikolskaya, and A. D. Mirzabekov.** 1991. Distribution of high mobility group proteins 1/2, E and 14/17 and linker histones H1 and H5 on transcribed and non-transcribed regions of chicken erythrocyte chromatin. Nucleic Acids Res. **19:**717–725.
63. **Richardson, K. K., J. Fostel, and T. R. Skopek.** 1983. Nucleotide sequence of the xanthine guanine phosphoribosyl transferase gene of *E. coli*. Nucleic Acids Res. **11:**8809–8816.
64. **Rideout, W. M., III, P. Eversole-Cire, C. H. Spruck III, C. M. Hustad, G. A. Coetzee, F. A. Gonzales, and P. A. Jones.** 1994. Progressive increases in the methylation status and heterochromatinization of the *myoD* CpG island during oncogenic transformation. Mol. Cell. Biol. **14:**6143–6152.
65. **Ridsdale, J. A., and J. R. Davie.** 1987. Selective solubilization of β-globin oligonucleosomes at low ionic strength. Biochemistry **26:**290–295.
66. **Riggs, A. D., and G. P. Pfeifer.** 1992. X-chromosome inactivation and cell memory. Trends Genet. **8:**169–174.
67. **Rivedal, E., and T. Sanner.** 1980. Synergistic effect on morphological transformation of hamster embryo cells by nickel sulphate and benz[a]pyrene. Cancer Lett. **8:**203–208.
68. **Sakai, T., J. Toguchida, N. Ohtani, D. W. Yandell, J. M. Rapaport, and T. P. Dryja.** 1991. Allele-specific hypermethylation of the retinoblastoma tumor-suppressor gene. Am. J. Hum. Genet. **48:**880–888.
69. **Salnikow, K., S. Cosentino, C. Klein, and M. Costa.** 1994. Loss of thrombospondin transcriptional activity in nickel-transformed cells. Mol. Cell. Biol. **14:**851–858.
70. **Sambrook, J., E. F. Fritsch, and T. Maniatis.** 1989. Molecular cloning: a laboratory manual, 2nd ed. Cold Spring Harbor Laboratory Press, Cold Spring Harbor, N.Y.

71. **Selker, E. U.** 1990. DNA methylation and chromatin structure: a review from below. Trends Biochem. Sci. **15:**1033–1037.
72. **Sen, P., K. Conway, and M. Costa.** 1987. Comparison of the localization of chromosome damage induced by calcium chromate and nickel compounds. Cancer Res. **47:**2142–2147.
73. **Sen, P., and M. Costa.** 1985. Induction of chromosomal damage in Chinese hamster ovary cells by soluble and particulate nickel compounds: preferential fragmentation of the heterochromatic long arm of the X-chromosome by carcinogenic crystalline NiS particles. Cancer Res. **45:**2320–2325.
74. **Stone-Wolff, D. S., C. B. Klein, and T. G. Rossman.** 1985. HGPRT− mutants of V79 cells that revert specifically by base pair substitution and frameshift mutations. Environ. Mutagen. **7:**281–291.
75. **Sutcliffe, J. S., D. L. Nelson, F. Zhang, M. Pieretti, C. T. Caskey, D. Saxe, and S. T. Warren.** 1992. DNA methylation represses FMR-1 transcription in fragile X syndrome. Hum. Mol. Genet. **1:**397–400.
76. **Swain, J. L., T. A. Stewart, and P. Leder.** 1987. Parental legacy determines methylation and expression of an autosomal transgene: a molecular mechanism for parental imprinting. Cell **50:**719–727.
77. **Tasseron-de Jong, J. G., H. den Dulk, P. van de Putte, and M. Giphart-Gassler.** 1989. *De novo* methylation as major event in the inactivation of transfected herpesvirus thymidine kinase genes in human cells. Biochim. Biophys. Acta **1007:**215–223.
78. **Thacker, J.** 1981. The chromosomes of a V79 Chinese hamster line and a mutant subline lacking HPRT activity. Cytogenet. Cell Genet. **29:**16–25.
79. **Tkeshelashvili, L. K., T. M. Reid, T. J. McBride, and L. A. Loeb.** 1993. Nickel induces a signature mutation for oxygen free radical damage. Cancer Res. **53:**4172–4174.
80. **Vogelstein, B., E. R. Fearon, S. E. Kern, S. R. Hamilton, A. C. Preisinger, Y. Nakamura, and R. White.** 1989. Allelotype of colorectal carcinomas. Science **244:**207–211.
81. **Weith, A.** 1983. Mg^{2+}-dependent compactness of heterochromatic chromosome segments. Exp. Cell. Res. **146:**199–203.
82. **Wigler, M. H.** 1981. The inheritance of methylation patterns in vertebrates. Cell **24:**285–286.
83. **Zhang, Y., T. Shield, T. Crenshaw, Y. Hao, T. Moutlon, and B. Tycko.** 1993. Imprinting of human H19: allele-specific CpG methylation, loss of the active allele in Wilm's tumor, and potential for somatic allele switching. Am. J. Hum. Genet. **53:**113–124.